Scientific Research Publishing

Open Journal of Applied Sciences, 2026, 16(11), 4534-4546
https://www.scirp.org/journal/ojapps
ISSN Online: 2165-3925
ISSN Print: 2165-3917

Loss Minimization and Voltage Profile Improvement Using AC Optimal Power Flow in a Constrained Transmission Network: A Real-Grid Case Study in the Democratic Republic of Congo

Seraphin Kasemuana Matototo, Vinny Loemba Vang-Si, Noel Zangio Tchioor Muyimp, Denis Tshiyoyo Nzengu, Adolphe Konifo Ngana

Higher Institute of Applied Techniques (ISTA), Kinshasa, Democratic Republic of the Congo
Email: Seraphin.kasemuana@ista.ac.cd

How to cite this paper: Matototo, S.K., Vang-Si, V.L., Muyimp, N.Z.T., Nzengu, D.T. and Ngana, A.K. (2026) Loss Minimization and Voltage Profile Improvement Using AC Optimal Power Flow in a Constrained Transmission Network: A Real-Grid Case Study in the Democratic Republic of Congo. *Open Journal of Applied Sciences*, **16**, 4534-4546.
https://doi.org/10.4236/ojapps.2026.1611248

Received: October 15, 2026
Accepted: November 17, 2026
Published: November 20, 2026

Copyright © 2026 by author(s) and Scientific Research Publishing Inc.
This work is licensed under the Creative Commons Attribution-NonCommercial International License (CC BY-NC 4.0).
http://creativecommons.org/licenses/by-nc/4.0/

Open Access

Abstract

This paper investigates the efficiency of AC optimal power flow (AC-OPF) for minimizing transmission losses and improving voltage profiles in a constrained, interconnected power system in the Democratic Republic of Congo. A reduced 17-bus, 19-branch representation of the western transmission system is developed using MATLAB/MATPOWER. The Newton-Raphson load flow establishes the reference operating condition, and an interior-point AC-OPF approach optimizes network operation subject to generation, voltage, and branch-flow constraints. To assess the sensitivity of the optimization results, we study two voltage-control ranges. The reference operating condition shows 54.44 MW active power losses and a minimum voltage of 0.9181 p.u. AC-OPF reduces losses to 48.20 MW (11.45%) and increases the minimum voltage to 0.9787 p.u. under the 0.90 - 1.10 p.u. voltage range. The losses are reduced to 51.78 MW (4.88%) within a narrower range of 0.93 - 1.07 p.u. The voltage is minimum at 0.9426 p.u. The branch-level analysis shows that 84.4% of the reference losses are concentrated in two major transmission corridors, and the southern transfer corridor dominates the optimization benefit. The results show that AC-OPF success in constrained transmission networks depends not only on the optimization algorithm but also on corridor properties and allowed voltage-control margins. The study provides a practical foundation for prioritizing operational optimization and targeted network reinforcement.

Keywords

AC Optimal Power Flow, Transmission Losses, Voltage Profile, Constrained

Transmission Network, Democratic Republic of Congo

1. Introduction

Electric power transmission systems must satisfy ever-increasing demand, long-distance bulk power transfers and cross-border exchanges while maintaining acceptable voltage profiles, thermal loading and generation limits. These problems are especially acute in constrained networks where transmission reinforcement does not keep pace with demand growth and where large power transfers are concentrated on a few corridors. Under these circumstances, improving the use of existing network assets can help reduce technical losses and mitigate voltage deterioration while longer-term reinforcement investments are being developed.

Optimal power flow (OPF) is a systematic framework for finding an operating point that minimizes a given objective function under nonlinear power flow equations and technical operating constraints. The roots of modern OPF can be traced to the work of Dommel and Tinney [1], who formulated the coordinated adjustment of power-system control variables to minimize operating cost or losses subject to network constraints. Later developments have produced many different solution techniques, including Newton-based, interior-point, evolutionary, convex-relaxation, and hybrid methods. An early comprehensive classification of OPF approaches was provided by Huneault and Galiana [2]. Subsequently, Frank *et al*. [3] [4] showed the variety of OPF formulations and solution methodologies developed for generation, transmission, and distribution applications.

Loss minimization and voltage-profile control are especially important when the network has limited operating margins. Sun *et al*. [5] proposed a Newton-based OPF method for constrained power-system optimization, providing a significant foundation for efficient nonlinear OPF computation. More recent formulations have extended the traditional OPF to incorporate voltage-security constraints and other optimization techniques. For example, Mohamed and Venkatesh [6] proposed a line-wise OPF formulation that considers voltage stability constraints and highlighted the importance of voltage security in network optimization. However, much of the current methodological research still presents new OPF formulations and algorithms mostly on standardized test systems, where the focus is often on computational performance, convergence, or optimality rather than on the operational characteristics of a specific constrained transmission system.

Benchmark networks are required to reproduce and compare optimization algorithms. Benchmark networks do not consider all operational features that exist in real transmission systems. The IEEE PES PGLib-OPF Task Force showed that even AC-OPF algorithm comparisons vary with network data, loading conditions, generation assumptions, and mathematical formulations, justifying the need for

standardized OPF benchmark cases [7]. MATPOWER also provides a widely used transparent environment for power-flow and OPF analysis that allows reproducible studies from small test systems to large networks [8]. However, benchmark-based results do not reflect an OPF strategy's performance when losses, voltage weaknesses, and bulk power transfers concentrate in a few strategic corridors of a real transmission network.

African power system studies also underline the importance of optimization and diverse modeling approaches. Oladeji and Oyinlola [9] analyzed the optimal operation of Nigeria's Ikeja West 132 kV sub-transmission network using Newton power flow and optimization to minimize transmission losses and improve voltage performance. Their work also included genetic-algorithm-based capacitor placement. But the analysis was on a sub-transmission system and compensation planning, not on loss-minimizing AC-OPF on a constrained bulk transmission network. Simplified network representations have been used in other African system-planning studies. For instance, Falchetta *et al*. [10] used an optimal power-flow-based framework to study transmission expansion under future electricity demand in Ethiopia. The work focused on long-term grid expansion and demand scenarios rather than the steady-state loss-minimizing operation of an existing constrained transmission system.

These studies suggest a more specific research gap. Published evidence on the performance of loss-minimizing AC-OPF on transmission-network representations from utilities operating under Central African conditions of concentrated long-distance power transfers, weak receiving-end voltages, high corridor losses, and restricted operational margins remains scarce. Moreover, knowing only the aggregate reduction in system losses does not tell us whether the improvement is due to generation redistribution, voltage-control action, relief of critical corridors, or operation close to control limits. If OPF results are to support operational decisions rather than serve only as numerical demonstrations, assessing these mechanisms is essential.

This paper addresses this gap by presenting a real-grid case study of a constrained, interconnected transmission network in the Democratic Republic of Congo. The reduced 17-bus, 19-branch AC representation preserves the major generation centers, load centers, transmission corridors, and regional interchange interfaces of the study system. First, the base operating condition is solved using Newton-Raphson power flow, then a loss-minimizing AC-OPF is implemented in MATLAB/MATPOWER using an interior-point solver. MATPOWER is selected for its transparent AC power-flow and OPF formulations and explicit support for generator, voltage, branch-flow, and other operating constraints [8].

Voltage-band sensitivity is examined through two completed operating cases; load-growth analysis is reserved for future work.

Section 2 formulates the network and AC-OPF problem; Section 3 describes the simulated cases; Section 4 discusses system and corridor results; Sections 5 and 6 present implications and conclusions.

2. Real-Grid Model and AC-OPF Problem Formulation

2.1. Study Network and Model Representation

The study system is a reduced 17-bus, 19-branch AC network extracted from an interconnected transmission network in the western region of the Democratic Republic of Congo. The model includes major generation centers, major urban and industrial load centers, strategic transmission corridors, and regional interchange interfaces. Downstream distribution loads are aggregated at representative transmission buses electrically. This reduction preserves the main active and reactive power exchanges that govern the system steady-state behavior and keeps the network computationally tractable for power flow and optimization studies.

The network comprises mainly 220, 132, and 70 kV transmission and subtransmission facilities, presented in per-unit on a 100-MVA base. Bus 1 is the slack bus, Bus 10 is a PV bus for the second generation center, and the other buses are PQ buses. The model consists of two modeled generation centers with a total maximum active power capacity of 1431 MW. The total modeled active-power demand, including the regional power transfer interfaces, is 1367.51 MW. The original study has the voltage limits set to 0.90 - 1.10 p.u.

The network representation includes two regional interchange interfaces. One is a major outgoing power transfer corridor to the southern interconnected system. The second is an external interchange with the neighboring system. These interfaces are retained as they have a major impact on the loading, losses, and voltage conditions of the study network. The geographical names of the main buses are preserved to maintain the electrical interpretation of the results, while the network's institutional identity and data status are used here to interpret the modeled network interfaces. The network reduction uses a functional aggregation approach, allocating downstream demand to representative transmission buses and explicitly modeling the main generation nodes, electrically significant transmission branches, and regional interchange points. The equivalent maintains the electrical characteristics of the preserved corridors and their associated active and reactive power exchanges, rather than replacing the entire interconnected system with a lumped transfer. In particular, the connection between the Inga and the southern system (Bus 1 - 16) and the receiving-end Bus 16 are preserved to account for the long-distance transfer and its effect on transmission losses and voltage magnitude. The model also represents the main western transmission paths to evaluate their relative contributions to network losses. This modeling approach allows attributing losses to corridors and identifying weak-voltage buses in the reduced network. The quantitative results are specific to the adopted 17-bus equivalent.

Table 1 summarizes the main technical characteristics of the reduced transmission network, including its configuration, generation capacity, modeled demand, and operating voltage limits.

Table 1. Key features of the study network.

Parameter	Model characteristic
Number of buses	17
Number of branches	19
System base	100 MVA
Main voltage levels	220/132/70 kV
Generation centers	2
Maximum modeled generation	1431 MW
Modeled active demand/transfers	1367.51 MW
Slack bus	Bus 1
PV bus	Bus 10
Voltage limits	0.90 - 1.10 p.u

2.2. AC Power-Flow Model

The Newton-Raphson AC power-flow formulation is used to establish the base operating condition. For each bus i, the complex power balance is expressed in terms of the bus-voltage magnitudes V_i, voltage angles θ_i, and elements $G_{ij} + jB_{ij}$ of the network admittance matrix. The active and reactive power balance equations are:

$$P_i = V_i \sum_{j=1}^{N} V_j \left[G_{ij} \cos\left(\theta_i - \theta_j\right) + B_{ij} \sin\left(\theta_i - \theta_j\right) \right] \quad (1)$$

$$Q_i = V_i \sum_{j=1}^{N} V_j \left[G_{ij} \sin\left(\theta_i - \theta_j\right) + B_{ij} \cos\left(\theta_i - \theta_j\right) \right] \quad (2)$$

At each bus, the net injected powers satisfy

$$P_i = P_{Gi} - P_{Di}, \quad Q_i = Q_{Gi} - Q_{Di} \quad (3)$$

where P_{Gi} and Q_{Gi} are the generator active and reactive power, and P_{Di} and Q_{Di} are the corresponding demands.

Since the present work is interested in both the active-power losses and voltage-magnitude performance, the nonlinear AC formulation is maintained, *i.e.*, the Newton-Raphson solution of (1)-(3) is used instead of a DC approximation. These quantities are functions of the coupled active and reactive power balance, voltage magnitudes, and the network impedance characteristics as represented by the full AC equations. While recent efforts have focused on developing computationally efficient OPF approximations and hybrid formulations for meshed networks [11], the full AC representation is still applicable when voltage constraints and transmission losses are major performance indicators [8] [12].

2.3. Loss-Minimizing AC-OPF Formulation

Operational or structural measures to mitigate transmission losses include reac-

tive-power control, voltage regulation, network reconfiguration, and optimized power dispatch. Recent work shows that topology reconfiguration can redirect transmission power flows and reduce transmission line losses while meeting voltage and operating requirements [13]. In the present study, however, the network topology is kept unchanged. The aim is to quantify the loss reduction and voltage improvement achievable through operational optimization (*i.e.*, adjusting the available control variables) before considering physical network reinforcement or reconfiguration.

The AC-OPF problem is to find a feasible operating point of the network that minimizes the active transmission losses, subject to the nonlinear AC power-flow equations and operational constraints. The optimization variables are generator active power, generator reactive power, voltage magnitudes, and voltage angles,

$$X = \left[\theta, V, P_G, Q_G\right]^{\mathrm{T}} \tag{4}$$

The active total transmission loss is calculated as for a network with N_L branches

$$P_{loss} = \sum_{(i,j)\in N_L} \left(P_{ij} + P_{ji}\right) \tag{5}$$

where P_{ij} and P_{ji} are the active-power flows measured at the two ends of branch $i-j$.

Hence, the optimization objective can be formulated as

$$\min f\left(x\right) = P_{loss} \tag{6}$$

The nonlinear equality constraints are the active- and reactive-power balance equations at each bus:

$$P_{Gi} - P_{Di} - P_i\left(V,\theta\right) = 0 \tag{7}$$

$$Q_{Gi} - Q_{Di} - Q_i\left(V,\theta\right) = 0 \tag{8}$$

with this formulation, the optimizer can find an operating condition that reduces power dissipated in the transmission network without reducing the specified demand.

2.4. Operational Constraints and Solution Method

The optimization is subject to generator capability, bus-voltage, and network operating limits. Generator active and reactive power outputs satisfy

$$P_{Gi}^{min} \le P_{Gi} \le P_{Gi}^{max}, \tag{9}$$

$$Q_{Gi}^{min} \le Q_{Gi} \le Q_{Gi}^{max}, \tag{10}$$

where the bus-voltage magnitudes are limited by

$$V_i^{min} \le V_i \le V_i^{max}. \tag{11}$$

For voltage limits, $V_i^{min} = 0.90$ p.u. and $V_i^{max} = 1.10$ p.u. Branch apparent-power flows are constrained by their respective thermal ratings,

$$\left|S_{ij}\right| \le S_{ij}^{max} \tag{12}$$

MATPOWER implements the loss-minimization objective using a linear generation-cost formulation, with the same marginal coefficients for the two generating units. For fixed demand and regional interchange conditions, the active-power balance requires that total generation equals supplied demand plus network losses. Thus, minimizing the total active-power generation is mathematically equivalent to minimizing the total transmission losses. This formulation allows the standard AC-OPF formulation to express the loss-minimization objective as in Eq. (6) without adding a nonlinear objective function.

The AC-OPF problem was solved using the primal-dual interior-point method in MATPOWER 7.1 [8] [14]. Numerical convergence was verified by checking the Karush-Kuhn-Tucker (KKT) optimality conditions, which include primal feasibility, stationarity, complementarity, and convergence of the objective function. In the C1 operating scenario, convergence was reached at 14 iterations with final residuals of (6.84 \times 10^{−7}), (1.40 \times 10^{−7}), (1.09 \times 10^{−7}), and (4.75 \times 10^{−7}), respectively. All four residuals were smaller than (10^{-6}), showing satisfactory numerical convergence and adherence to the prescribed optimality criteria. The results verify the numerical accuracy of the optimal operating point and its compliance with the network operating constraints. Because the AC-OPF is nonconvex, the solution is only a locally optimal operating point, not a globally optimal one.

This work does not propose a new optimization algorithm; it evaluates the operational value and physical limitations of loss-minimizing AC-OPF on a constrained real-grid representation. Recent research has proposed alternative, computationally efficient OPF formulations [11] [12]. However, it is useful to retain a well-established AC-OPF formulation to help interpret the resulting generator dispatch, voltage-control actions, branch flows, and binding constraints.

3. Simulation Framework and Cases

The 17-bus transmission network was analyzed using Newton-Raphson AC load flow to establish the reference operating condition (A0), followed by AC-OPF under two voltage-control ranges. The first optimized case (A1/C1) uses the original voltage limits of 0.90 - 1.10 p.u., while the second case (A2/C2) uses a tighter range of 0.93 - 1.07 p.u. All simulations retain the same network topology, specified demand of 1367.51 MW, generator capability limits, and branch ratings. The performance assessment considers active-power losses, minimum bus voltage, generator dispatch, branch-loss concentration, and operating constraints. The tighter voltage range is introduced to evaluate optimization sensitivity rather than represent a specific regulatory requirement.

The computational model is in MATPOWER case format and includes bus demands, branch electrical parameters and ratings, generator capability limits, and generation-cost coefficients. The simulation procedure includes Newton-Raphson reference load flow and AC-OPF calculations for the two investigated voltage-control ranges. The cases share the same network topology, demand, and genera-

tion limits, so the observed differences reflect the operating constraints and optimization decisions investigated.

4. Results and Discussion

4.1. Reference-State Diagnosis and Loss Concentration

At A0, total active generation is 1421.95 MW against 1367.51 MW of modeled demand and interchange, producing 54.44 MW of active losses and 109.28 MVAr of reactive losses. Bus 16, at the receiving end of the southern transfer interface, has the lowest voltage (0.9181 p.u.). Losses are strongly concentrated: branch 1 - 16 dissipates 35.12 MW (64.5% of system losses) and branch 1 - 3 dissipates 10.85 MW (19.9%). Together they represent approximately 84.4% of the reference active losses. Their prominence shows that system-wide loss mitigation must focus on the dominant transfer paths, not just the total loss figure.

Figure 1 shows the distribution of active-power losses across the principal transmission corridors, revealing that branches 1 - 16 and 1 - 3 contribute most to the total reference losses.

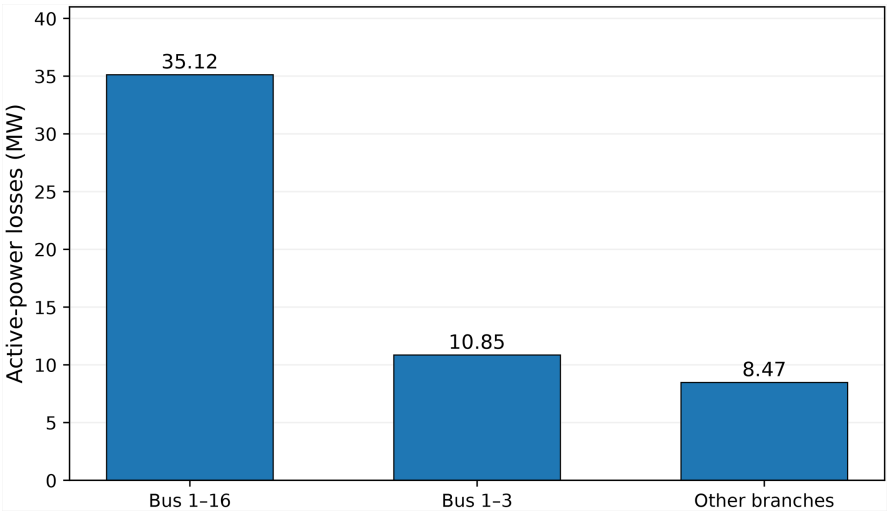


Figure 1. Reference loss concentration in the principal corridors.

4.2. AC-OPF Performance and Voltage-Limit Sensitivity

For C1, active losses fall to 48.20 MW, a saving of 6.24 MW (11.45%), and the minimum voltage rises to 0.9787 p.u. at Bus 16. For C2, losses are 51.78 MW, giving a 2.66-MW saving (4.88%), while the minimum voltage is 0.9426 p.u. at Bus 16. Hence, narrowing the voltage band reduces the loss saving by 3.58 MW and lowers the minimum optimized voltage by 0.0361 p.u. Relative to A0, however, C2 still achieves measurable improvement in both indicators. The optimized slack-bus voltage reaches its upper permitted limit in both cases (1.1000 p.u. for C1; 1.0700 p.u. for C2), showing that the upper voltage constraint is a consequential control restriction in these solutions.

The reference operating condition A0 meets the original voltage range of 0.90 -

1.10 p.u., but its minimum voltage of 0.9181 p.u. is below C2's lower limit of 0.93 p.u. So A0 is not possible with the tighter voltage requirements of C2. The 4.88% loss reduction obtained in C2 is then understood when considering the original operating condition and the recovery of compliance with the tighter voltage limits. Conversely, comparing C1 and C2 isolates the effect of the allowed voltage-control range on the optimized operating losses.

Table 2 compares the principal operating indicators from the reference load flow (A0) and the two optimized cases (C1 and C2), highlighting how voltage constraints affect transmission losses and minimum bus voltage.

Table 2. Summary of reference and optimized operating conditions.

Indicator	A0: load flow	C1: AC-OPF	C2: AC-0PF
Voltage band (p.u.)	0.90 - 1.10	0.90 - 1.10	0.93 - 1.07
Generation (MW)	1421.95	1415.71	1419.29
Active losses (MW)	54.44	48.20	51.78
Loss reduction (%)	-	11.45	4.88
Minimum voltage (p.u)	0.9181	0.9787	0.9426
Minimum voltage bus	16	16	16

Figure 2 illustrates the nodal voltage profiles under the reference and optimized operating conditions, showing improved performance at weak buses and the influence of the two voltage-control ranges.

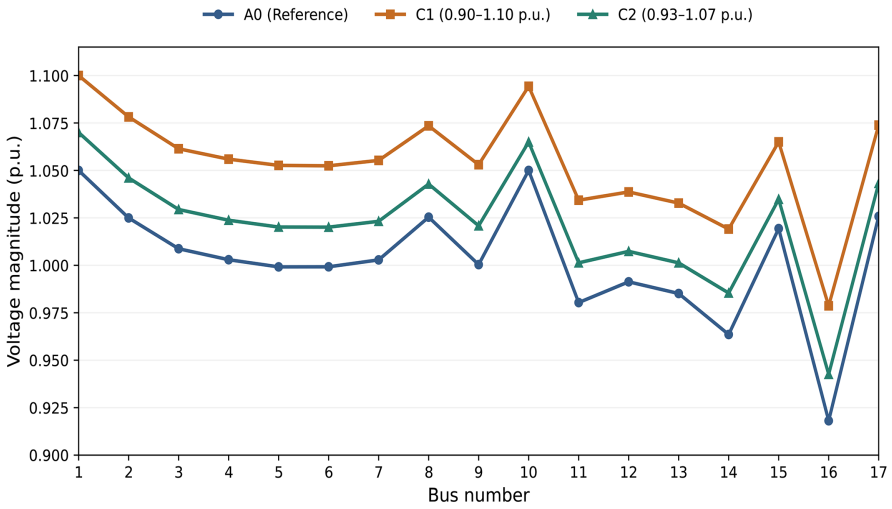


Figure 2. Nodal voltage profiles for A0, C1, and C2.

Figure 3 compares the total active-power losses in cases A0, C1, and C2, showing the reduction achieved through AC-OPF and how sensitive these savings are to tighter voltage constraints.

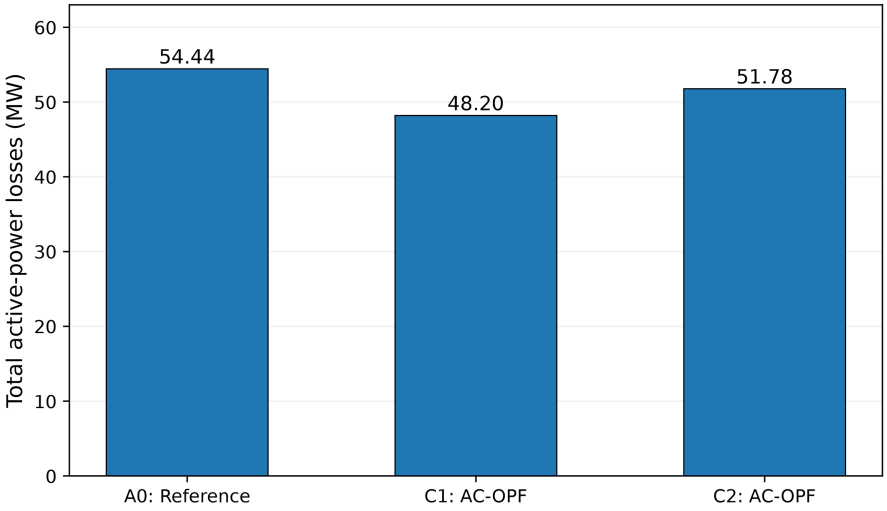


Figure 3. System active losses under the reference and two voltage-band cases.

4.3. Operational Interpretation and Cross-Platform Check

The optimized operating conditions show the combined effect of generation dispatch and voltage regulation on the transmission losses. Total active generation decreases from 1421.95 MW in A0 to 1415.71 MW in C1 and 1419.29 MW in C2, while modeled demand remains constant at 1367.51 MW. In C1, the second generation center is operating at the active-power ceiling of 131 MW, and the slack-bus voltage is at the upper permitted limit of 1.10 p.u. C2 limits the upper voltage limit of the slack bus to 1.07 p.u., thus limiting the voltage control range. These operating conditions justify the wider voltage range, allowing greater loss reduction, and the narrower voltage range, limiting potential improvement. The results highlight how generator operating constraints, voltage regulation, and transmission-corridor characteristics interact to define the optimized operating point.

The reference operating condition was also compared with a DIgSILENT load-flow representation, which yielded 58.99 MW of active-power losses, whereas MATPOWER yielded 54.44 MW. The 4.55 MW difference is about 7.7% of the DIgSILENT result and comparable to loss savings achieved by optimization. This discrepancy shows that the two reference representations are not numerically identical without detailed reconciliation of their component parameters, network equivalents, and operating assumptions. Thus, the cross-platform comparison provides only an estimate of the general magnitude of reference losses, not direct validation of the optimized solution. The reported loss reductions are calculated consistently in the same MATPOWER network model, with unchanged topology, demand, and interchange conditions.

Table 3 presents the individual active- and reactive-power outputs and voltage magnitudes of the Inga and Zongo generating units under the reference (A0) and optimized (C1 and C2) operating conditions, together with the identified binding operating constraints.

Table 3. Generator operating conditions and identified binding constraints under A0, C1 and C2.

Case	Generator bus	Pg (MW)	Qg (MVAr)	Voltage (p.u.)	Identified binding constraint
A0	1 (Inga)	1290.95	420.43	1.0500	Reference operating condition
A0	10 (Zongo)	131.00	59.48	1.0500	Active-power upper limit
C1	1 (Inga)	1284.72	386.06	1.1000	Upper voltage limit
C1	10 (Zongo)	131.00	49.94	1.0943	Active-power upper limit
C2	1 (Inga)	1288.29	408.88	1.0700	Upper voltage limit
C2	10 (Zongo)	131.00	52.93	1.0650	Active-power upper limit

Table 3 shows that the Inga generator active power output decreases from 1290.95 MW in A0 to 1284.72 MW in C1 and 1288.29 MW in C2, while the Zongo generator stays at its 131 MW active power limit. Thus, the corresponding reductions in total generation come from adjustments at the Inga generator, consistent with the observed transmission-loss savings under fixed demand. Reactive power generation also decreases for both generators, with the largest reduction at C1. The Inga bus voltage rises from 1.0500 p.u. in A0 to its upper allowed limits of 1.1000 p.u. in C1 and 1.0700 p.u. in C2, respectively. These results indicate that voltage regulation, rather than active-power redistribution between the two generators, is the primary observed control change associated with loss of minimization. The binding Zongo active-power limit and Inga voltage limits further demonstrate how generator capability and voltage-control constraints shape the optimal operating points.

5. Practical Implications and Study Boundaries

The comparison shows that voltage-control freedom is an operational resource for reducing resistive losses, particularly at heavily loaded, long-distance transfer interfaces. The C1 benefit occurs at the upper slack-bus voltage bound; therefore, it should not be interpreted as a universally achievable saving under tighter voltage requirements. The study represents balanced steady-state operation on an aggregated network and does not establish N-1 security, dynamic voltage stability, time-varying feasibility, or the implementability of every modeled control action. These are boundaries of the present scope, rather than additional simulated outcomes.

6. Conclusions and Future Research

This study investigated the effectiveness of loss-minimizing AC-OPF in improving operating efficiency and voltage performance in a constrained, interconnected transmission network in the Democratic Republic of Congo. The results show that operational optimization can achieve tangible improvements without altering the current network topology or reducing the specified demand. Active-power loss

decreases from 54.44 MW to 48.20 MW (an 11.45% reduction) in the 0.90 - 1.10 p.u. voltage range, and the minimum voltage increases from 0.9181 to 0.9787 p.u. The loss reduction is 4.88%, and the minimum voltage is 0.9426 p.u. in the tighter range of 0.93 - 1.07 p.u.

The main scientific contribution is identifying the relationship between transmission loss concentration, voltage-control flexibility, and achievable AC-OPF benefits in a constrained real-network representation. Two major transmission branches account for about 84.4% of the reference active-power losses. The southern transfer corridor accounts for about 67.5% of the total loss reduction. Furthermore, the achievable loss reduction is limited by the reduced voltage-control range, indicating that operational optimization efficiency depends on both network characteristics and allowed operating constraints. These results provide the basis for identifying where operational control is most effective, and where targeted network reinforcement may provide additional benefits.

The analysis will be extended in future work to progressive demand growth scenarios, N-1 security constraints, reactive power capability sensitivity and multi-period operating conditions. Particular emphasis will be placed on the determination of loadability limits of the existing network and the comparison of operational optimization with targeted reinforcement of the dominant transmission corridors.

Author Contributions

Seraphin Kasemuana Matototo conceived the paper, drafted the theoretical framework, and supervised the overall preparation of the manuscript, including the technical approach, application analysis, and interpretation of the results. Vinny Loemba Vang-Si, Noel Zangio Tchioor Muyimp, Denis Tshiyoyo Nzengu, and Adolphe Konifo Ngana conducted the simulations and prepared the results. All authors reviewed and approved the final manuscript.

Conflicts of Interest

The authors declare no conflicts of interest regarding the publication of this paper.

References

[1] Dommel, H. and Tinney, W. (1968) Optimal Power Flow Solutions. *IEEE Transactions on Power Apparatus and Systems*, **87**, 1866-1876. https://doi.org/10.1109/tpas.1968.292150

[2] Huneault, M. and Galiana, F.D. (1991) A Survey of the Optimal Power Flow Literature. *IEEE Transactions on Power Systems*, **6**, 762-770. https://doi.org/10.1109/59.76723

[3] Frank, S., Steponavice, I. and Rebennack, S. (2012) Optimal Power Flow: A Bibliographic Survey I. *Energy Systems*, **3**, 221-258. https://doi.org/10.1007/s12667-012-0056-y

[4] Frank, S., Steponavice, I. and Rebennack, S. (2012) Optimal Power Flow: A Bibliographic Survey II. *Energy Systems*, **3**, 259-289.

https://doi.org/10.1007/s12667-012-0057-x

[5] Sun, D., Ashley, B., Brewer, B., Hughes, A. and Tinney, W. (1984) Optimal Power Flow by Newton Approach. *IEEE Transactions on Power Apparatus and Systems*, **103**, 2864-2880. https://doi.org/10.1109/tpas.1984.318284

[6] Mohamed, A.A. and Venkatesh, B. (2019) Voltage Stability Constrained Line-Wise Optimal Power Flow. *IET Generation*, *Transmission & Distribution*, **13**, 1332-1338. https://doi.org/10.1049/iet-gtd.2018.5452

[7] Babaeinejadsarookolaee, S., *et al*. (2019) The Power Grid Library for Benchmarking AC Optimal Power Flow Algorithms. arXiv: 1908.02788.

[8] Zimmerman, R.D., Murillo-Sanchez, C.E. and Thomas, R.J. (2011) MATPOWER: Steady-State Operations, Planning, and Analysis Tools for Power Systems Research and Education. *IEEE Transactions on Power Systems*, **26**, 12-19. https://doi.org/10.1109/tpwrs.2010.2051168

[9] Ifedayo, R.O. and Aminat, O.O. (2017) Operation Optimization of Ikeja West Power Subtransmission Network in a Deregulated Market Environment. 2017 *IEEE* 3*rd International Conference on Electro-Technology for National Development* (*NIGERCON*), Owerri, 7-10 November 2017, 987-993. https://doi.org/10.1109/nigercon.2017.8281964

[10] Juturu, P., Conlon, T., Zhang, Y., Avraam, C., Siddiqui, S., Simane, B., *et al*. (2023) Optimal Grid Expansion under Future Electricity Demand for Groundwater Irrigation in Ethiopia. *Energy for Sustainable Development*, **72**, 351-377. https://doi.org/10.1016/j.esd.2022.12.006

[11] Esmaeel Nezhad, A., Nardelli, P.H.J., Javadi, M.S., Jowkar, S., Tavakkoli Sabour, T. and Ghanavati, F. (2025) A Hybrid Optimal Power Flow Model for Transmission and Distribution Networks. *Electric Power Systems Research*, **245**, Article ID: 111638. https://doi.org/10.1016/j.epsr.2025.111638

[12] Altorok, M., Ukil, A., Nair, N.C. and Rayudu, R. (2024) Review on Optimal Power Flow in a Hybrid AC/DC Distribution Network. *Electric Power Systems Research*, **236**, Article ID: 110956. https://doi.org/10.1016/j.epsr.2024.110956

[13] Orbea, D., Carrión, D. and Jaramillo, M. (2025) Minimization of Transmission Line Losses through System Topology Reconfiguration. *Energies*, **18**, Article 2063. https://doi.org/10.3390/en18082063

[14] Wang, H., Murillo-Sanchez, C.E., Zimmerman, R.D. and Thomas, R.J. (2007) On Computational Issues of Market-Based Optimal Power Flow. *IEEE Transactions on Power Systems*, **22**, 1185-1193. https://doi.org/10.1109/tpwrs.2007.901301